School of Optometry, University of California at Berkeley, Berkeley, CA, USA

School of Optometry, University of California at Berkeley, Berkeley, CA, USA

School of Optometry, University of California at Berkeley, Berkeley, CA, USA

The detectability and appearance of visual targets can be modulated by surround stimuli. In this study we asked how cross- and iso-oriented surrounds modulate contrast detection and discrimination in foveal vision. We systematically measured the Threshold-versus-Contrast (TvC) functions over a wide range of pedestal and surround contrasts. Our results show that cross-oriented surrounds lower the contrast threshold over the entire range of pedestal and surround contrasts, but iso-surround modulation of the TvC function is dependant on the relative contrast, being facilitative when the surround/pedestal contrast ratio $C_{sur}/C_{ped} < 1$ and suppressive when $C_{sur}/C_{ped} > 1$. Data fitting indicates that cross-surround modulation (facilitation) is mainly due to improved gain, except at very low and high surround contrasts. Iso-surround modulation on the other hand is more complicated, probably reflecting more than one surround process as determined by the relative contrast.

Keywords: surround modulation, cross-orientation, iso-orientation, Stromeyer-Foley d' function, TvC function, classical receptive fields

The responses of V1 neurons can be modulated by stimulation outside the neurons' classical receptive fields (e.g., Hubel & Wiesel, 1965; Nelson & Frost, 1985; Knierim & Van Essen, 1992; Kapadia, Westheimer, & Gilbert, 2000; etc). This surround or contextual modulation indicates that V1 neurons are not simply isolated bar and edge detectors. Instead they interact with each other with a potential for serving more complex visual functions. Among various issues of surround modulation studied by researchers in both neurophysiology and psychophysics are the roles of relative surround orientation, ranging from collinear (iso) to orthogonal (cross). In neurophysiological studies, surround facilitation and suppression have been reported at both iso and cross surround orientations (Hubel & Wiesel, 1965; Nelson & Frost, 1985; Knierim & Van Essen, 1992; DeAngelis, Freeman, & Ohzawa, 1994; Kapadia, Ito, Gilbert, & Westheimer, 1995; Sillito, Grieve, Jones, Cudeiro, & Davis, 1995; Toth, Rao, Kim, Somers, & Sur, 1996; Das & Gilbert, 1999; Hupe, James, Girard, & Bullier, 2001; Jones, Wang, & Sillito, 2002). The results are not always consistent, but the relative stimulus contrast has been cited as one important factor to account for some of the controversies about whether surrounds produce facilitation or suppression (Kapadia et al., 2000).

At the psychophysical (visual system) level, the influences of surround stimuli on contrast detection and discrimination may also provide insights into the surround modulation issue (e.g., Dresp, 1993; Polat & Sagi, 1993; Zenger & Sagi, 1996; Snowden & Hammett, 1998; Solomon, Watson, & Morgan, 1999; Yu & Levi, 2000). Collinear or iso-surround modulation has been studied most often (e.g., Polat & Sagi, 1993; Zenger & Sagi, 1996; Yu & Levi, 1997; Snowden & Hammett, 1998; Solomon et al., 1999), but only a small number of studies have investigated psychophysical surround modulation by cross-surround stimuli (Raasch, 1988; Polat & Sagi, 1993; Yu & Levi, 1998, 2000; Chen & Tyler, 2002; Yu, Klein, & Levi, 2002).

Strong cross-surround facilitation of contrast detection was demonstrated by Yu, Klein and Levi (2002), both with annular surround stimuli (replotted in this paper, Figure 3, top left panel) and with Gabor flankers similar to those used by Polat and Sagi (1993). Similar effects were first reported in a thesis by Raasch (1988). Yu, et al. (2002) found that cross-surround facilitation of contrast detection is surround-contrast dependent. It mainly manifests at low surround contrasts but not at high surround contrasts, which explains why no cross

DOI 10:1167/3.8.1 Received January 15, 2003, published September 25, 2003 ISSN 1534-7362 © 2003 ARVO

facilitation was evident in Polat and Sagi (1993). Control measurements by Yu, et al. (2002) showed that cross-surrounds facilitate contrast detection mainly by improving the internal signal/noise ratio rather than by reducing stimulus uncertainty.

For contrast discrimination, Yu and Levi (2000) reported two distinct types of surround effects, one narrowly tuned to iso-orientation, and the other broadly tuned to cross-orientation. Surround modulation of contrast discrimination at cross- and iso-orientations for a fixed pedestal contrast (0.40) is generally facilitative, but with distinct contrast dependencies. Cross-surrounds at contrasts higher than the pedestal contrast produce stronger facilitation that could completely eliminate masking. In contrast, iso-surround facilitation is diminished when the surround contrast is higher than the pedestal contrast.

In the current study we expanded our investigation to systematically study cross- and iso-surround modulation over a broad range of pedestal and surround contrasts by measuring complete threshold versus contrast (TvC) functions at multiple surround contrasts. We also fit the data quantitatively using a variant of the standard contrast-response function (which we call the Stromeyer-Foley function) to examine how the underlying contrast response function is modulated by cross- and iso-surrounds. Our experiments and data fitting enable us to test conclusions of previous researchers based on data collected from limited stimulus conditions, and to obtain a better understanding of psychophysical cross- and iso-surround modulation.

Three adult observers with normal or corrected-to-normal vision served in the study. BJ and ND were new to psychophysical observation and received several sessions of training. YC, one of the authors, was highly experienced.

The stimuli (Figure 1) were generated by a VisionWorks computer graphics system (Vision Research Graphics, Inc., Duham, NH) and presented on a U.S. Pixel Px19 monochrome monitor (1024 x 512 resolution, 0.28 mm (H) x 0.41 mm (V) pixel size, 117 Hz frame rate, 62 cd/m^2 mean luminance, and 3.8^o x 3.0^o screen size at the 5.64-meter viewing distance). Luminance of the monitor was made linear by means of a 15-bit look-up table. Experiments were run in a dimly lit room.

The target (Figure 1) was a 10 arcmin long spatially localized D6 grating (the sixth derivative of a Gaussian, T in Figure 1b) centered in-phase on a circularly windowed sinusoidal grating pedestal (P in Figure 1b) of the same spatial frequency (8.0 cpd) and orientation (vertical) with contrast varying from 0 to 0.40. The D6 target (similar to a Gabor function with σ = 4.1 arcmin) was multiplied by a Gaussian window along its long axis (σ = 4.2 arcmin) and truncated at the target length. The size of the circular pedestal was larger than the target (d = 18 arcmin), which would maximize masking at high pedestal contrasts (Yu & Levi, 1997, 2000) because of a desensitization effect (Westheimer, 1967), but would change masking very little at low pedestal contrasts because desensitization at low pedestal contrasts is nearly negligible (Westheimer, 1967). The surround (S in Figure 1b) was a sinusoidal grating annulus abutting the pedestal with contrast varying from 0 to 0.80. The outer and inner diameters of the surround were 45 and 18 arcmin, respectively. Contrast thresholds were measured with a successive two-alternative forced-choice staircase procedure. The pedestal was presented in each of the two stimulus intervals (300 msec each) separated by a 400 msec inter-stimulus interval. Each stimulus interval was accompanied with an audio tone of the same duration. The target was randomly presented in one of the two stimulus intervals with the same onset and offset as the pedestal. The observers' task was to judge which stimulus interval contained the target. Each trial was preceded by a 6.3' x 6.3' fixation cross which disappeared 100 msec before the beginning of the trial. Audio feedback was given on incorrect responses. Each staircase consisted of four preliminary reversals and eight experimental reversals. The step size of contrast change in preliminary reversals was 7.5% of the previous contrast

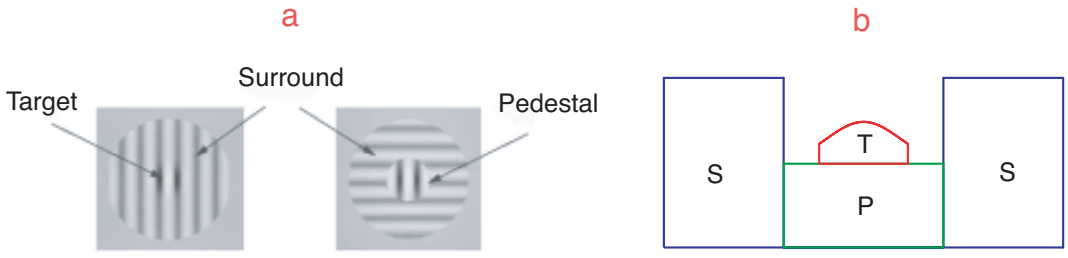

Figure 1. Stimuli. The stimuli consisted of a D6 grating target centered on a circularly windowed sinusoidal grating pedestal. The pedestal was abutted by an annular sinusoidal grating surround. (a) Iso-surround (left) and cross-surround (right) conditions. (b) The stimulus profile at the x-axis. T is the D6 target, P is the pedestal, and S is the surround grating.

and in experimental reversals it was 2.5%. Each correct response lowered the target contrast by one step and each incorrect response raised the target contrast by three steps, which resulted in a 75% convergence level of the staircase. The mean of the eight experimental reversals was taken as the contrast threshold. Each datum represents the mean of 5-6 replications, and the error bars represent +/−1 standard error of the mean.

Each experimental session typically consisted of three segments lasting for approximately two hours. Each segment measured one TvC function (six staircases for six pedestal contrasts at C_{ped} = 0 to 0.40 in a random order). TvC functions at different surround orientations (cross and iso) and contrasts (C_{sur} = 0 to 0.80) were measured in a balanced order.

Our results show that cross-oriented surrounds lower the contrast threshold over the entire range of pedestal and surround contrasts, but iso-surround modulation of the TvC function is dependant on the surround/pedestal contrast ratio (C_{sur}/C_{ped}), being facilitative when $C_{sur}/C_{ped} \leq 1$ and suppressive when $C_{sur}/C_{ped} > 1$. These effects are evident in Figures 2 -4.

Figure 2 shows the TvC functions of the mean data from three observers and data fitting outputs (see later Data Fitting section) (cross-surround data in the left column and iso-surround data in the right column). The error bar for each datum represents either the average of the three corresponding individual error bars, or the standard errors of individual thresholds, whichever is larger. Each row shows cross- and iso-surround TvC functions at one surround contrast (in ascending order from 0.025 to 0.80), as well as the baseline TvC function (C_{sur} = 0). Individual data and data fitting outputs can be retrieved by clicking here.

The mean and individual baseline functions (i.e., the TvC function with no surround shown by black asterisks and dashed lines replicated in each panel) resemble a typical TvC function (e.g.,Legge & Foley, 1980). As the pedestal contrast increases, the contrast threshold first decreases and then increases, forming a dipper near the detection threshold.

Cross-surrounds facilitate the entire TvC function at all surround contrasts (red circles). At low and moderate surround contrasts (C_{sur} = 0.05 to 0.40), especially at C_{sur} = 0.10 & 0.40, facilitation is mainly due to a downshift of the TvC function. At the lowest surround contrast (C_{sur} = 0.025), facilitation is minimal at detection (C_{ped} = 0), most evident at the dipper (C_{ped} = 0.025 ~ 0.10), and weakens as the pedestal contrast increases (which results in a steeper slope of the TvC function at high pedestal contrasts). At the highest surround contrast (C_{sur} = 0.80), facilitation is mainly evident at high pedestal contrast with little effect at low pedestal contrasts, and the TvC function is flatter at high pedestal contrasts.

Iso-surrounds facilitate the entire TvC function at the lowest surround contrast (C_{sur} = 0.025) except for detection (C_{ped} = 0) (blue circles). As the surround contrast increases, facilitation is limited to higher pedestal contrasts, and iso-surround modulation at lower pedestal contrast becomes suppressive, raising thresholds above the baseline when C_{sur} = 0.80. The transition from suppression to facilitation appears to be determined by the relative contrast of the surround and pedestal (considered below). At C_{sur} = 0.40, suppression changes to facilitation dramatically, producing a kink in the TvC function at high pedestal contrasts. At the highest surround contrast (C_{sur} = 0.80), suppression is evident at low pedestal contrasts (C_{ped} <= 0.1) with thresholds equal to the baseline at C_{ped} = 0.20 and 0.40.

Several interesting properties emerge when the mean cross and iso data are plotted together (replotted from Figure 2) at each pedestal contrast as a function of the surround contrast (Figure 3 – lower abscissa). First, at higher pedestal contrasts (C_{ped} = 0.10 ~ 0.40), cross- and iso-surrounds produce nearly identical facilitation when $C_{ped} > C_{sur}$ (values less than 1 on the top abscissa, which shows the ratio of surround to pedestal contrast). Similar data reported previously at C_{ped} = 0.40 (Yu & Levi, 2000) are also included (Figure 3, bottom right). However, iso facilitation diminishes when $C_{ped} < C_{sur}$, suggesting the influence of the relative contrast of pedestal and surround stimuli (see below).

Second, at lower pedestal contrasts, although cross facilitation tends to be strong, iso surrounds do not have much effect on contrast thresholds, except for slight facilitation at the lowest contrasts (C_{sur} = 0.025) and some suppression when the surround contrast is much higher than the pedestal contrast (C_{sur} = 0.80). Lack of surround modulation at lower pedestal contrast, especially at detection, is specific to the annular iso-surround stimuli we used, as significant iso-facilitation is evident when collinear flankers restricted to near the ends of a target stimuli are used (e.g., Polat & Sagi, 1993).

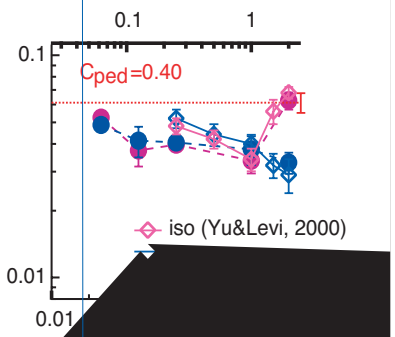

ng and cross

m *ped*

, these common mechanisms prod

Cross and iso surround modulation can be summarized by plotting normalized mean contrast thresholds (i.e. threshold-with-surround/threshold-with-no-surround) against the surround/pedestal contrast ratio (C_{sur}/C_{ped}) (Figure 4). Clearly, cross-surrounds facilitate regardless of C_{sur}/C_{ped}, though facilitation tends to be stronger at a lower C_{sur}/C_{ped}. On the other hand, iso-surround modulation is dependent on C_{sur}/C_{ped}. As C_{sur}/C_{ped} increases, iso-surround modulation changes from facilitation to suppression. Iso-surrounds mainly produce facilitation when $C_{sur}/C_{ped} \leq 1$ and suppression when $C_{sur}/C_{ped} > 1$.

In order to fit the TvC data we used a contrast response function (the *d'* function, Stromeyer & Klein, 1974; Legge & Foley, 1980; Foley, 1994; Boynton, Demb, Glover, & Heeger, 1999; Chen & Tyler, 2001) to fit TvC data. This function can be written as:

$$d'(C) = \frac{KC^{p}}{(C_k^{\,p-w} + C^{p-w})}. \quad (1)$$

We call this *d'* contrast response function the Stromeyer-Foley function, in which C is the stimulus contrast, p is the log-log slope at low contrast, w is the log-log slope at high contrast, C_k is the contrast at the kink point where lines drawn through the high and low asymptotes intersect as seen in Figure 6a, and K controls the height of the function. A deeper exploration of the role each of the parameters plays in controlling the shape of the *d'* function and the TvC function is taken up in the Appendix.

The parameters of the *d'* function can be determined from contrast discrimination data such as shown in Figure 2. The connection between the *d'* function and the TvC function is given by:

$$d'(C_{ped} + C_{test}) - d'(C_{ped}) = 1 \quad (2)$$

where C_{ped} is the pedestal contrast and C_{test} is the test threshold in a contrast discrimination task.

When C_k is small compared to C as for the present data, Equation 1 becomes:

$$d'(C) \cong KC^{w} \quad (3)$$

Thus, K is approximately the *d'* value at 100% contrast. The connection of K to the high contrast Weber fraction is derived by keeping the leading terms of the Taylor's expansion of Equations 2 and 3, based on the assumption that $C_{test} << C_{ped}$.

$$1 = K((C_{ped} + C_{test})^{w} - C_{ped}^{w}) \approx Kw\, C_{ped}^{w-1}\, C_{test} \quad (4)$$

So the Weber fraction is given by:

$$C_{test}/C_{ped} = 1/(Kw\, C_{ped}^{w}) \quad (5)$$

At $C_{ped} = 1$ the Weber fraction is simply $1/Kw$. Equations 4 and 5 also illustrate that the log-log slope of the TvC function (C_{test} as a function of C_{ped}) is $1-w$. Thus the high contrast portion of the TvC function pins down the parameters K and w. A full understanding of the connection between C_{test} and C_{ped} in the TvC function depends on many factors including the nature of the underlying transducer function, the amount of uncertainty, early and late gain control, and the amount of additive and multiplicative noise. We present a simplified model of visual processing which includes each of these factors in the Appendix (Figure 7); for the present, we fit the data with the four parameter Stromeyer-Foley function and look for systematic changes in the parameters produced by the iso and cross surrounds. In particular, we are interested in whether the Stromeyer-Foley function can account for the surround effects on the basis of parameter changes, or whether additional factors need to be included.

We first used Equation 1 to fit cross-surround effects. The cross TvC functions at all six surround contrasts were fitted simultaneously via a nonlinear least square method (the Matlab lsqnonlin function). To reduce the number of parameters, we experimented by letting one parameter be a single value (the same for all surround contrast conditions) and the other three parameters be vectors (different values for different surround contrast conditions). The total number of parameters was 3*6+1 = 19. The number of data points being fit was 36. The goodness of the fit, chi square (χ^2), was the lowest (χ^2 = 28.4, df = 17) when p was a single value. The χ^2 was reduced when all four parameters were allowed to float (χ^2 = 23.2), but the values of parameters became unstable due to the high correlation between p and other parameters. In addition, the reduction of chi square from 28.4 to 23.2 was insufficient to justify the five extra parameters.

The fitted values of K, C_k, and w are plotted against the surround contrast in Figure 5 (p has a single value across the six surround contrasts), as are values of $1/wK$ (approximately the Weber fraction at C = 1.0 as shown in Equation 5). The error bars on the parameters estimates are based on the variance output by the lsqnonlin program (without making the reduced chi square

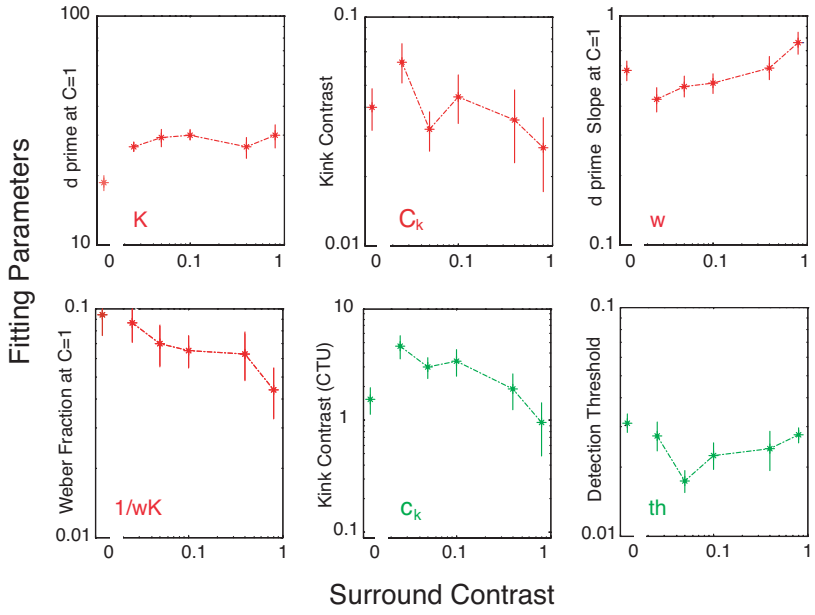

Figure 5. Fitting results for cross modulation data using Equation 1. The three parameters K, w, C_k and the combination *1/wK* are shown as functions of the surround contrast. The fourth parameter p in the data fitting was constrained to be the same value at all cross surround contrasts (p=2.27). See Appendix for explanations of the additional panels *(c_k & th).* CTU: Contrast threshold unit

heterogeneity correction), except for error bars of 1/*wK* that were calculated with a Monte Carlo simulation based on the standard errors of *w* and *K*. The *d'* functions associated with these parameter values are also shown (Figure 6).

The Stromeyer-Foley function generally captures the properties of cross surround modulation (Figure 2, left column, solid red lines) quite well. As shown in Figure 5, *K* is nearly equally raised at all surround contrasts, indicating that a cross surround at any (visible) contrast improves the gain. A more detailed analysis in the Appendix will show that a raised *K* vertically lifts the Stromeyer-Foley function. However, such a gain change could occur at different stages of visual processing (Node 3 or 7 of Figure 7), so the exact mechanism underlying gain change cannot be unequivocally determined. The gain improvement is clearly a dominant effect of cross surround modulation at C_{sur} = 0.1~ 0.4. At very low and

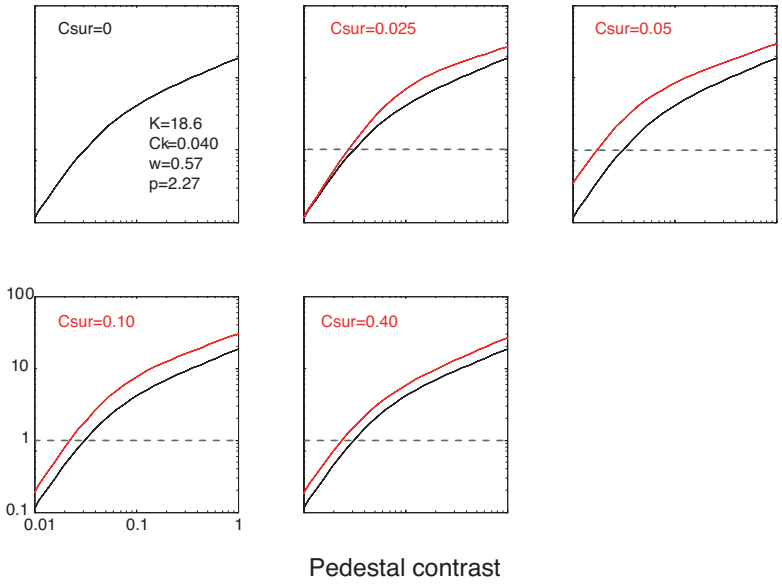

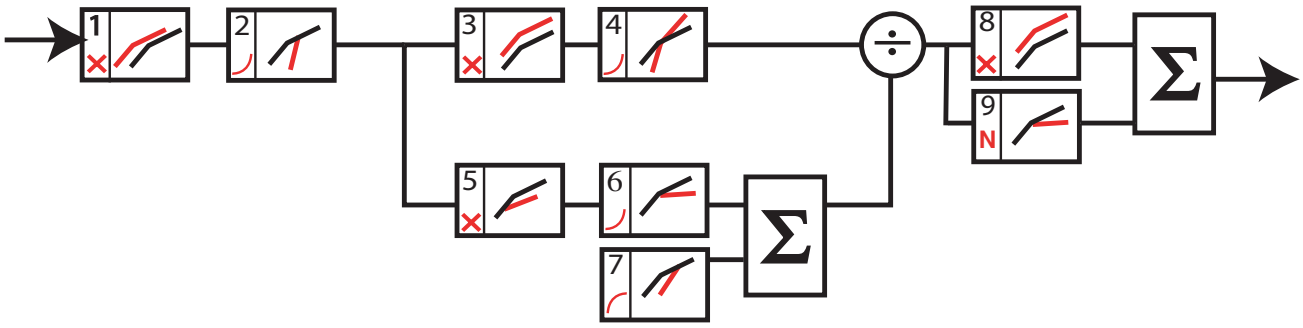

Figure 7. A simplified model of visual processing. The icon on the lower left of each node represents the action of that node as discussed in the text. The broken lines in each node represent the S-F function. The shift in the broken lines (from black to red) shows how surround modulation at that node would shift the S-F function. The black lines are identical across all nodes.

high contrasts (C_{sur} =0.05 and 0.8), the cross surround also changes the kink contrast (C_k) and the high-contrast slope *w*. A change of C_k may indicate a change of pooled divisive inhibition (node 7 in Figure 7) as discussed in the Appendix. And a change of w may indicate a change of saturation or gain control of the transducer function (node 6 in Figure7), or stimulus dependent multiplicative noise (node 9 in Figure 7), or both. Finally, Figure 5 also indicates that the high contrast Weber fraction, $1/wK$, is a smoothly decreasing function of surround contrast. Because *K* is fairly constant, this change is mainly contributed by *w* that increases as a function of surround contrast.

The fitted curves often miss the data points at the 0.10 pedestal contrast when $C_{sur} \geq 0.10$, where the fits indicate more facilitation than is evident in the actual data. This discrepancy may be due to individual differences (it is only true for the two novice observers but not for the highly practiced author). However, if this is a genuine effect reflecting additional suppression near $C = C_{ped} = 0.10$ (possibly reducible with learning), it can be simulated by adding a subtractive component $(-a*(1+0.125/C)^{-2})$ to the Stromeyer-Foley function (Figure 2, left column, dotted green lines). The parameter values in this new component were chosen to give a decent fit of suppression near $C_{ped} = 0.1$. They were chosen by a rough trial and error procedure, since there are not enough data points to constrain data fitting.

Unlike cross-surround data fitting, iso-surround data fitting is more qualitative than quantitative. First we attempted to use Equation 1 to fit the iso-surround data, and the same fitting procedure as for cross-surround data was followed. Although fitting was reasonably good for iso TvC functions at C_{sur} = 0.025, 0.05 as well as at C_{sur} = 0.80 (Figure 2, right column, dotted blue lines), Equations 1 and 2 do not capture the suppression-to-facilitation transition at high pedestal contrasts of the iso TvC function at C_{sur} = 0.40. Fitting for the iso TvC function at C_{sur} = 0.10 also misses the dipper when the slope of the TvC function at high pedestal contrasts is satisfied.

Earlier we pointed out that iso-surround effects are nearly identical to cross-surround effects when $C_{sur} < C_{ped}$. When $C_{sur} > C_{ped}$ there is not much iso modulation except some facilitation at the lowest surround contrast and suppression at the highest surround contrast. That is, iso-surround effects appear to be primarily a two-state function, and which state they are in is determined by the relative contrast. To demonstrate this, we combined the segments of the baseline fitting curve at $C_{ped} < C_{sur}$ and the cross fitting curve at $C_{ped} > C_{sur}$ and plotted them together with the iso TvC data in Figure 2. The specific rules for the combination require an assumption about what to do near the transition point when $C_{ped} = C_{sur}$: The perceptual matching point of the center and surround will depend on their overall contrast. At low contrasts the surround's perceived contrast is expected to be larger than the pedestal's because of the larger size of the surround. We measured the detection thresholds for the pedestal and for the surround for subject YC and found the pedestal threshold to be 1.3 times the surround threshold. At high contrasts the perceived contrast of the center and surround are expected to be equal. Because of this effect of perceived contrast, in Figure 2 when $C_{sur} \leq 0.10$ the $C_{ped} = C_{sur}$ point was grouped with $C_{ped}<C_{sur}$ (the perceived contrast of the pedestal was reduced because of its smaller size). When $C_{sur} > 0.10$, the $C_{ped} = C_{sur}$ point was grouped with $C_{ped}>C_{sur}$. For example, at C_{sur} = 0.05, we combine the baseline curve up to C_{ped} = 0.05 and cross curve starting at C_{ped} = 0.10, leaving a gap between C_{ped} = 0.05 and C_{ped} = 0.10. However at C_{sur} = 0.40, we combine the baseline curve up to C_{ped} = 0.20 and cross curve starting at C_{ped} = 0.40, leaving a gap between C_{ped} = 0.20 and C_{ped} = 0.40. Figure 2 right column shows that a combination of baseline fits (thick black lines) and cross fits (thick red lines) nicely account for most of the iso data. The exception is the extra inhibition

seen at the highest surround contrast (C_{sur} = 0.80), probably as a result of multiplicative noise induced by high-contrast surround stimuli (discussed below).

In this study we systematically measured cross- and iso-surround modulation of the TvC function over a wide range of surround contrasts. Cross-surround facilitation is evident across the entire TvC function. Iso-surround modulation of the TvC function is dependent on the relative contrast (C_{sur}/C_{ped}), being facilitative when $C_{sur}/C_{ped} \leq 1$ and suppressive when $C_{sur}/C_{ped} > 1$. Data fitting indicates that cross-surround modulation (facilitation) can be reasonably accounted for by changes in the Stromeyer-Foley *d'* function, mainly a raised gain, except at very low and high surround contrasts. Iso-surround modulation on the other hand is more complicated, probably reflecting more than one process and is affected by the relative contrast.

Constraining the explanations for surround modulation. Our experimental results and data fitting suggest that surround modulation of contrast response is a complex process and is influenced by the surround contrast (cross) or relative contrast (iso). The contrast response function is varied differently by surrounds at different contrasts. This complexity is not captured by many previous (including our own) studies in which limited surround contrasts (often a single surround contrast) are used (e.g., Snowden & Hammett, 1998; Chen & Tyler, 2001). In these studies, results are often simpler and can be more smoothly fit to support authors' models. The trade-off is that these models may not be properly constrained and have limited application.

The original motive of the current study, as well as many other studies, is to pin down the underlying (psychophysical) mechanisms of surround modulation. However, this worthwhile goal is compromised by the complex nature of visual processing. As the Appendix details, multiple mechanisms at different stages of visual processing could be responsible for the change of a single parameter in the *d'* function. For example, a raised gain due to cross surround modulation could equally possibly occur at different stages of visual processing, even within the frame of our simple model. Similarly, a reduced high-contrast slope of the TvC function (1-*w*) could indicate either a change of saturation or gain control of the transducer, or increased stimulus dependent multiplicative noise. These multiple possibilities suggest that data fitting does not provide sufficient power to fully constrain the psychophysical mechanisms of surround modulation.

On the other hand, data fitting does help discount some possible mechanisms and constrain the explanation. Specific to our cross data, we can eliminate two possible explanations. First, nice fits are obtained with a single *p* (the low-contrast slope) across surround contrasts. A change of p would indicate a change of uncertainty due to cross surround modulation. Indeed, the effects of cross-surrounds seen in Figure 2 do not resemble the pattern seen in Figure 8b which simulates the TvC function changes that would occur if p varies. Thus it is unlikely that the surround produces facilitation through an uncertainty reduction mechanism. Elsewhere, we (Yu, Klein & Levi, 2002) provided experimental evidence that the cross facilitation of detection cannot be fully explained by uncertainty reduction. One of these arguments is that the bottom of the dipper of the unflanked TvC curve can be strongly facilitated by the cross-oriented surrounds (see Figure 2). Uncertainty reduction is unlikely to account for the surround's facilitation of the dipper regime since the presence of the

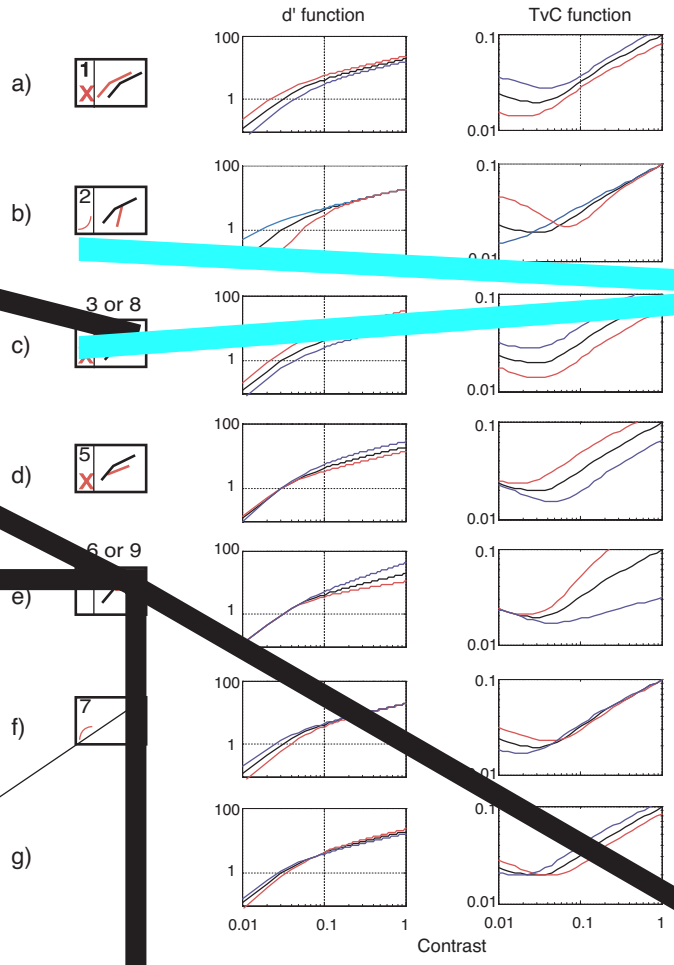

pedestal should have minimized the uncertainty so there wouldn't be any uncertainty for the surround to minimize.

Secondly, contrast masking is often attributed to pooled divisive inhibition （Malik & Perona, 1990; Heeger, 1992; Albrecht & Geisler, 1991; Foley, 1994). This divisive pooling varies the saturation point C_k in Equation 1 and shifts the log-log *d'* curve diagonally approximately in the direction of the high contrast slope (see Figure 8f). If cross surrounds modulate contrast responses by solely manipulating the gain control pool, it would effectively change the value of C_k in the denominator of Equation 1. However, our data fitting indicates that a significant change of the value of C_k only occurs at very low and high surround contrasts, discounting the single gain control pool idea as a full explanation for cross-surround modulation.

Our pedestals are slightly larger than the D6 target to approximately cover the full extent of the underlying receptive field center (or “perceptive field center” in a psychophysical sense) and to maximize masking (Westheimer, 1967; Yu & Essock, 1996; Yu & Levi, 1997). Thus, at high pedestal contrasts both cross- and iso- surround facilitation can be at least partially understood as variations of the Westheimer sensitization effect (Yu & Levi, 1997, 1998, 2000). That is, stimulation by a surround outside the perceptive field center coul8-1 1 Tf-0.00425.5799 Tm(YuMC/Span <</MCID27 T 5b3ection 8 Tm(, Thac

p being the slope of the log-log *d'* function at low pedestal contrasts. The parameters *K* and *w* are determined by the large pedestal contrast region of the TvC curve with 1-*w* being the log-log slope of the TvC function (see Equation 5) and 1/*Kw* being the test contrast for C_{ped} = 1.0 (see Equation 5) under the assumption that C_k <<1.0, as is typical for spatial frequencies below about 15 c/deg. For the parameters of the unflanked condition (see Figure 6), the jnd at a 100% pedestal (*C* = 1.0) is 1/*Kw* = 1/(18.6*0.57) = 0.094. A test contrast of 9.5% at a 100% pedestal gives a Weber fraction of 0.094, a reasonable value at high pedestal contrasts. Another way of looking at these numbers is that a 9.4% test contrast together with the high contrast TvC slope of *w* = 0.57 gives *K* = 1/(0.094*0.57) = 18.6. *K* is approximately the *d'* at C = 1.0. This means that there are approximately *K* = 19 jnds from zero contrast to 100% contrast.

The parameter C_k can be calculated from the parameters *th*, *p*, *K* and *w* using Equation 7. C_k can also be determined graphically by drawing two straight lines on the log-log *d'* function that match the high and low contrast asymptotic regions as shown in Figure 6a. C_k is the pedestal contrast where the two asymptotic lines intersect. It specifies the region where the *d'* slope changes from *p* to *w*.

How the four parameters of the S-F function are determined by the underlying visual processing

Figure 7 shows a simplified model of visual processing that consists of three stages: Early processing stage (Nodes 1 &2), intermediate processing stage including an excitatory branch (Nodes 3 & 4) and a divisive inhibitory branch (Nodes 5, 6 & 7), and an output stage (Nodes 8 & 9). Each of the nine nodes indicates where a nonlinearity or gain control process could be influenced by the surround. A detailed discussion of each node will be presented in conjunction with Figure 8; here we present an overview of the nodes. Nodes 1, 3, 5 and 8 represent gain control mechanisms where the signal gets multiplied by a constant, i.e. output = constant* input. Node 1 is in the early stage and affects threshold, th. Nodes 3 (excitatory branch of intermediate processing) and 8 (output), control the output scale factor, *K*. Node 5, in the divisive inhibitory branch of intermediate processing will be seen to affect the high contrast region of the *d'* function. Nodes 2, 4 and 6 correspond to power law nonlinearities in their respective branches of the model, i.e. output = input^{power}. Node 7 corresponds to an additive gain control that affects the saturation point of the divisive inhibition branch of the model. This node corresponds to the pooled gain control found in many models of cortical processing, as will be discussed. Node 9 is multiplicative output noise.

In the lower left corner of each node in Figure 7 is one of four symbols representing the action performed at that node: (a) An X (nodes 1, 3, 5 and 8) represents a gain control stage where the signal is multiplied by a constant. (b) An accelerating curve (nodes 2, 4 and 6) represents a nonlinearity where the output is a power function of the input ($y = x^a$). (c) A decelerating curve (node 7) represents a saturating stage. For example, the surround could contribute to a gain control pool that adds a constant to the denominator of the S-F function. Even without a surround there would be a semi-saturation constant contributing to the denominator. (d) A letter "N" (node 9) represents multiplicative noise at the output. The multiplicative nature of this noise will reduce the log-log slope of the *d'* function at high contrasts.

The right side of each node shows how the S-F function is altered at each node. The S-F function is represented by a broken line where the break is at C_k with the slopes of the two line segments given by *p* and *w*, and the height of the lines given by *K* or *th*. A pair of broken lines are shown in each node representing how the surround can alter the S-F function by modulating that node. The black lines are identical across all nodes and set the baseline, and red lines show how the S-F function is changed by surround influence. For a multiplicative node the surround would modify the gain at that stage. For a nonlinear node the surround would change the power exponent. For the additive gain control pooling node 7 the presence of the surround would give an additive contribution at that node. For the output noise node 9, the surround could suppress or enhance the noise. The division sign between nodes 4 and 8 represents the divisive inhibition typical of feed-forward gain control models.

We now discuss how a surround can modify specific parameters of the S-F function. To illustrate these effects Figure 8 shows separate nodes from Figure 7 (left panel) and associated plots of the S-F function (middle panels) and TvC function (right panels). The middle of the three curves in each S-F or TvC panel is the S-F or TvC function with parameters that best fit our unflanked averaged data: *p*=2.27, *w* = 0.57 (or *q* = *p*-*w* =1.70), *K*=18.4, C_k=0.040 (corresponding to *th* = 0.031 and c_k = 1.29). The other two curves shown in red and blue correspond to the S-F and TvC functions with specific model parameters decreased and increased by a factor of $\sqrt{2}$ except as discussed below.

Figure 8a shows the effect of a gain control modulation at node 1, producing a change in threshold, *th*, in Equation 6, while fixing *p*, *w*, and c_k. This manipulation of parameters shifts the *d'* curve horizontally. The TvC curve (right panel) shows a downward shift which is greater at low contrast than at high, similar to the effect of a low contrast cross surround as seen in the second and third panels of Figure 2 (also see Figure 6 for *d'* function change).

Figure 8b shows the effect of a modification in node 2. The main effect is to change *p*, the log-log slope at low contrast. The semi-saturation contrast, C_k is also altered. It is interesting that the high contrast portions of the S-F

contrasts when the surround contrast is high. This is precisely what is expected for the standard gain control (or noise intrusion) shown in Figure 8f.

As our final example, Figure 8g shows that by combining a shift downward plus an equal shift leftward one can produce an approximately leftward shift of the TvC function. This type of shift has been reported by Chen & Tyler (2001), but it is not seen in our data. There is an ambiguity as to which nodes are involved in producing the shifts seen in Figures 8g as well as 8a, c and d, since there are four nodes (1, 3, 5 and 8) that produce translations in different directions, but a general translation can be represented by just two parameters.

A similar ambiguity is present for the slope parameters, *p* and *w*. Node 4 just affects the slope of the branch in the numerator, thereby altering both the low and the high contrast slopes (not shown in Figure 8). Since there are four nodes (2, 4, 6, 9) that affect the two slope parameters, the present experiments are unable to pin down the nodes where the surround modifies the slope. As was discussed earlier in connection with Figure 5, the surround had minimal effect on *p* and only a small effect on *w*.

This research is supported by National Institute of Health grants 01E 01728 01E 04776. thank Alex Tauras for his help with constructing Figure 7. Commercial relationships: none.

Adini, Y., & Sagi, D. (2001). Recurrent networks in human visual cortex: psychophysical evidence. *Journal of Optical Society of America A, 18*, 2228-2236.[PubMed]

Albrecht, D. G., & Geisler, W. S. (1991). Motion selectivity and the contrast-response function of simple cells in the visual cortex. *Visual Neuroscience, 7*, 531-546.[PubMed]

Boynton, G. M., Demb, J. B., Glover, G. H., & Heeger, D. J. (1999). Neuronal basis of contrast discrimination. *Vision Research, 39*, 257-269.[PubMed]

Chen, C. C., & Tyler, C. W. (2001). Lateral sensitivity modulation explains the flanker effect in contrast discrimination. *Proceedings of the Royal Society of London. Series B: Biological Sciences, 268*, 509-516.[PubMed]

Chen, C. C., & Tyler, C. W. (2002). Lateral modulation of contrast discrimination: Flanker orientation effects. *Journal of Vision, 2*, 520-530.[Article]

Das, A., & Gilbert, C. D. (1999). Topography of contextual modulations mediated by short-range interactions in primary visual cortex. *Nature, 399*, 655-661.[PubMed]

DeAngelis, G. C., Freeman, R. D., & Ohzawa, I. (1994). Length and width tuning of neurons in the cat's primary visual cortex. *Journal of Neurophysiology, 71*, 347-374.[PubMed]

Dresp, B. (1993). Bright lines and edges facilitate the detection of small line targets. *Spatial Vision, 7*, 213-225.[PubMed]

Foley, J. M. (1994). Human luminance pattern-vision mechanisms: masking experiments require a new model. *Journal of the Optical Society of America A, 11*, 1710-1719.[PubMed]

Heeger, D. J. (1992). Normalization of cell responses in cat striate cortex. *Visual Neuroscience, 9*, 181-197.[PubMed]

Hubel, D. H., & Wiesel, T. N. (1965). Receptive fields and functional architecture in two nonstriate visual areas (18 and 19) of the cat. *Journal of Neurophysiology, 28*, 229-289.

Hupe, J. M., James, A. C., Girard, P., & Bullier, J. (2001). Response modulations by static texture surround in area V1 of the macaque monkey do not depend on feedback connections from V2. *Journal of Neurophysiology, 85*, 146-163.[Article]

Jones, H. E., Wang, W., & Sillito, A. M. (2002). Spatial organization and magnitude of orientation contrast interactions in primate v1. *Journal of Neurophysiology, 88*, 2796-2808.[Article]

Kapadia, M. K., Ito, M., Gilbert, C. D., & Westheimer, G. (1995). Improvement in visual sensitivity by changes in local context: Parallel studies in human observers and in V1 of alert monkeys. *Neuron, 15*, 843-856.[PubMed]

Kapadia, M. K., Westheimer, G., & Gilbert, C. D. (2000). Spatial distribution of contextual interactions in primary visual cortex and in visual perception. *Journal of Neurophysiology, 84*, 2048-2062.[Article]

Knierim, J. J., & Van Essen, D. C. (1992). Neuronal responses to static texture patterns in area V1 of the alert macaque monkey. *Journal of Neurophysiology, 67*, 961-980.[PubMed]

Kontsevich, L. L., Chen, C. C., & Tyler, C. W. (2002). Separating the effects of response nonlinearity and internal noise psychophysically. *Vision Research, 42*, 1771-1784.[PubMed]

Legge, G. E., & Foley, J. M. (1980). Contrast masking in human vision. *Journal of the Optical Society of America, 70*, 1458-1470.[PubMed]

Legge, G. E., Kersten, D., & Burgess, A. E. (1987). Contrast discrimination in noise. *Journal of the Optical Society of America A, 4*, 391-404.[PubMed]

Malik, J., & Perona, P. (1990). Preattentive texture discrimination with early vision mechanisms. *Journal of the Optical Society of America A, 7*, 923-932.[PubMed]

Nelson, J. I., & Frost, B. (1985). Intracortical facilitation among co-oriented co-axially aligned simple cells in cat striate cortex. *Experimental Brain Research, 61*, 54-61.[PubMed]

Polat, U., & Sagi, D. (1993). Lateral interactions between spatial channels: Suppression and facilitation revealed by later masking experiments. *Vision Research, 33*, 993-999.[PubMed]

Raasch, T. W. (1988). Lateral masking and enhancement with spatially-periodic visual stimuli. *University of California, Berkeley, Ph.D. dissertation*.

Sillito, A. M., Grieve, K. L., Jones, H. E., Cudeiro, J., & Davis, J. (1995). Visual cortical mechanisms detecting focal orientation discontinuities. *Nature, 378*, 492-496.[PubMed]

Snowden, R. J., & Hammett, S. T. (1998). The effects of surround contrast on contrast thresholds, perceived contrast and contrast discrimination. *Vision Research, 38*, 1935-1945.[PubMed]

Solomon, J. A., & Morgan, M. J. (2000). Facilitation from collinear flanks is cancelled by non-collinear flanks. *Vision Research, 40*, 279-286.[PubMed]

Solomon, J. A., Watson, A. B., & Morgan, M. J. (1999). Transducer model produces facilitation from opposite-sign flanks. *Vision Research, 39*, 987-992.[PubMed]

Stromeyer, C. F., & Klein, S. (1974). Spatial frequency channels in human vision as asymmetric (edge) mechanisms. *Vision Research, 14*, 1409-1420.[PubMed]

Toth, L. J., Rao, S. C., Kim, D., Somers, D., & Sur, M. (1996). Subthreshold facilitation and suppression in primary visual cortex revealed by intrinsic signal imaging. *Proceedings of the National Academy of Science, 93*, 9869-9874.

Westheimer, G. (1967). Spatial interaction in human cone vision. *Journal of Physiology, 190*, 139-154.[PubMed]

Yu, C., & Essock, E. A. (1996). Psychophysical end-stopping associated with line target. *Vision Research, 36*, 2883-2896.[PubMed]

Yu, C., Klein, S. A., & Levi, D. M. (2002). Facilitation of contrast detection by cross-oriented surround stimuli and its psychophysical mechanisms. *Journal of Vision, 2*, 243-255.[Article]

Yu, C., & Levi, D. M. (1997). End-stopping and length tuning in psychophysical spatial filters. *Journal of the Optical Society of America A, 14*, 2346 - 2354.[PubMed]

Yu, C., & Levi, D. M. (1998). Spatial frequency and orientation tuning in psychophysical end-stopping. *Visual Neuroscience, 15*, 585-595.[PubMed]

Yu, C., & Levi, D. M. (1999). The time course of psychophysical end-stopping. *Vision Research, 39*, 2063-2073.[PubMed]

Yu, C., & Levi, D. M. (2000). Surround modulation in human vision unmasked by masking experiments. *Nature Neuroscience, 3*, 724-728.[PubMed]

Zenger, B., & Sagi, D. M. (1996). Isolating excitatory and inhibitory nonlinear spatial interactions involved in contrast detection. *Vision Research, 36*, 2497-2513.[PubMed]

Zenger-Landolt, B., & Koch, C. (2001). Flanker effects in peripheral contrast discrimination--psychophysics and modeling. *Vision Research, 41*, 3663-3675.[PubMed]